



AERO-ELASTIC BEHAVIOR OF HIGH-RISE BUILDINGS UNDER DOWNSTREAM INTERFERENCE EFFECTS

Yuan-Lung LO

Dept. Civil Eng., Tamkang University – Taiwan

yllo@mail.tku.edu.tw

Yong Chul KIM

Dept. Architecture, Tokyo Polytechnic University – Japan

kimyc@arch.t-kougei.ac.jp

Akihito YOSHIDA

Dept. Architecture, Tokyo Polytechnic University – Japan

yoshida@arch.t-kougei.ac.jp

Abstract

This paper investigates the effect of the single and multiple aerodynamic modification mechanisms on the dynamic behaviour of the principal building when it is interfered by a very closely located building. During the study, aeroelastic vibration tests and high-frequency force balance tests are conducted to compare responses and wind forces in a well-simulated turbulent boundary layer flow. The principal building is manufactured with three different building configurations to represent the single and multiple aerodynamic modification treatments; the neighbouring building which produces interference effects is made as a square prism model. Results show that the multiple modification treatment is efficient in reducing wind forces in all interference location series. However, it is also found that in some critical conditions, such treatment is sensitive to reduced velocity and may amplify the interference effect and result in larger displacements.

INTRODUCTION

Interference effects caused by neighbouring buildings require an improved wind load resistant design rather than those for isolated buildings. However, due to their complex nature and huge number of disturbances, the interference effects have been considered very difficult in regulation coding for practical use. The issue with the interference effects is still one of the most difficult research topics in the field of wind engineering.

Over the past decades, researchers have adopted various methodologies to investigate the interference effects on overall or local wind loads of high-rise buildings. Factors that may affect the wind forces have been widely discussed, such as the approaching flow characteristics, wind directions, relative location of neighbouring buildings, cross sectional shapes and aspect ratios, Scruton numbers, Strouhal numbers, modal frequency, and mode shapes. Among these research works, square or rectangular prisms, as well as cylindrical prisms, chimneys, storage tanks, or cladding structures were commonly chosen for discussions. In most cases, interference effects were discussed based on the evaluation of distorted wind forces to indicate critical interference locations. However, it has been pointed out that different critical interference mechanisms could occur at certain interference locations, either at the upstream or the downstream, to generate significant responses (Bailey and Kwok, 1985;

Yahyai et al., 1992; Lo et al., 2016), especially in the area very close to the principal building. In related works, the aeroelastic vibration test was considered more intuitive to observe the interfered dynamic responses rather than high-frequency force balance tests.

On the other hand, the aerodynamic modifications that can efficiently reduce the wind force acting on high-rise buildings are reported in recent works. Changing the geometrical appearance of the building shape may be the easiest treatment among the aerodynamic modifications. Two simple but efficient treatments, changing the number of sides of the cross section and changing the helical angle to twist the building, are concluded to promise lower wind forces by Kim et al. (2014, 2015, and 2016). Surprisingly, these treatments sometimes happen to meet building designers' imagination and design of what symbol the buildings stand for. In the modern skyscraper designs, the taper and twisting features are becoming more and more attractive today.

This study intends to investigate the effects of the single and the multiple aerodynamic modification treatments on the interfered responses by the experimental results from aeroelastic vibration tests. The modifications are attempted to be achieved by manufacturing three principal models, including a square prism model, a taper model, and a helical taper model. Closed interference locations are selected to cover those critical interference mechanisms either from the upstream or the downstream. Response buffeting factors are estimated to examine how the treatments work to reduce or amplify the unfavourable dynamic behaviour of the target principal building.

EXPERIMENTAL SETTING

The aeroelastic vibration test is conducted in the $18 \times 1.8 \times 2.2$ m boundary layer wind tunnel of Wind Engineering Research Centre at Tokyo Polytechnic University. A 1/400 scale turbulent flow over a sub-urban terrain with a power law index exponent for mean velocity profile of 0.19 is simulated with properly equipped spires, saw barriers, and roughness blocks (Photo 1). The vertical flow characteristics are shown in Fig. 1.

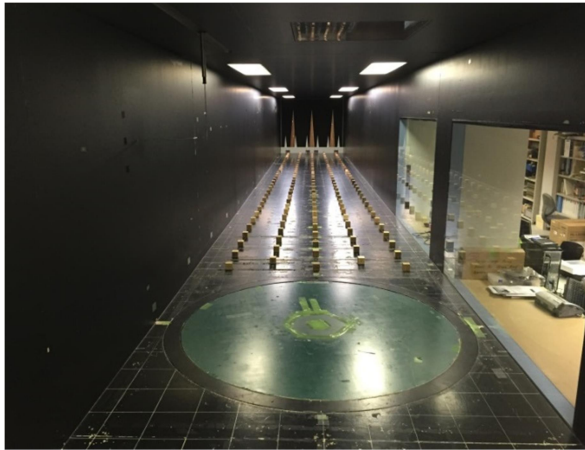


Photo 1 Wind tunnel at WERC, TPU

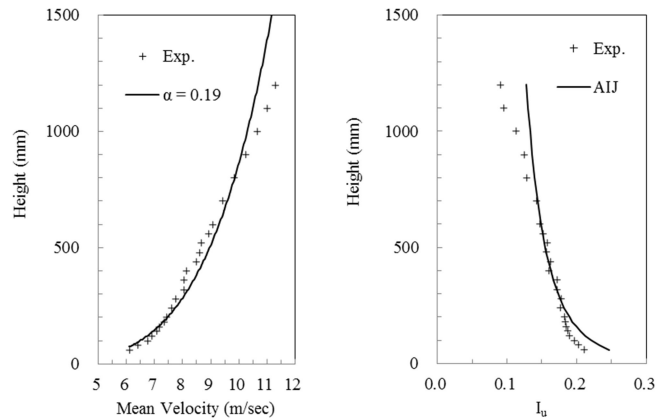
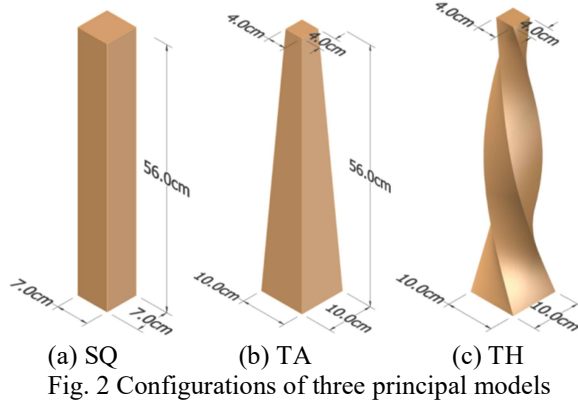


Fig. 1 Vertical profiles of simulated flow

Three rigid base-pivoted aero-elastic models are manufactured for the role of the principal building as shown in Fig. 2. The square prism model is 0.07 m in both width and depth and 0.56 m in height, which make the aspect ratio 8. The tapered model is 0.04 m in width on the roof-top and 0.10 m in width on the bottom. The height is the same as the square one and the aspect ratio (height to the averaged width) is also 8. The helical tapered model has the same geometrical appearance as the tapered model but has a helical twisting angle of 180° from the bottom to the top. All the three principal models are manufactured with the same volume in order to have a basic comparison level. Both the tapered and the helical tapered models have been proven to efficiently reduce the projected wind force when they are considered in an isolated condition (Kim et al., 2014, 2015, 2016). The tapered model and the helical tapered model in this study are also referred to Model IV and X by Kim

et al. (2016). The setup of the aeroelastic vibration test is illustrated in Fig. 3. The reason to choose the tapered and the helical tapered models in this study is that the buildings with tapered shape and twisting features are becoming more and more attractive in the modern skyscraper designs; however, the associated discussions have not been widely made for such two features. It is also the authors' interest to investigate the consequences with the consideration of interference effects.



(a) SQ (b) TA (c) TH
Fig. 2 Configurations of three principal models

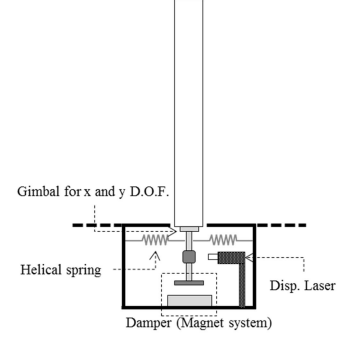


Fig. 3 Diagram of vibration test

Table 1 Fundamental information of three principal models

Principal model	Square (SQ)	Tapper (TA)	Helical tapper (TH)
Height (H)	0.56	0.56	0.56
Depth (D)	0.07	0.10 (bottom) 0.04 (top)	0.10 (bottom) 0.04 (top)
Width (B)	0.07	0.10 (bottom) 0.04 (top)	0.10 (bottom) 0.04 (top)
H/B_{ave}	8	8	8
Helical angle	0°	0°	180°
$f_{n,x}$ (Hz)	6.5	6.5	6.5
$f_{n,y}$ (Hz)	6.5	6.5	6.5
ζ_x (%)	0.8	0.7	1.0
ζ_y (%)	0.9	0.8	1.0
M^* (g)	107	111	111
δ_x	0.25	0.23	0.32
δ_y	0.30	0.27	0.33

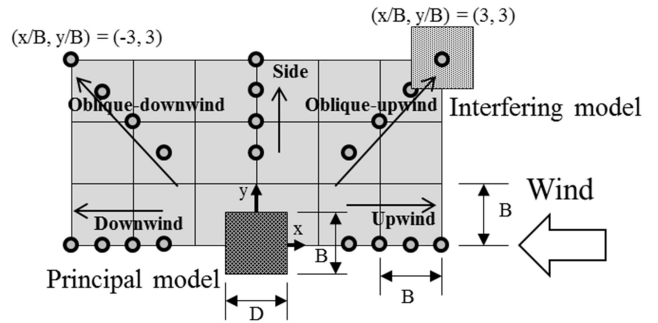


Fig. 4 Interference locations

Table 2 Neglected cases with the number of distorted records larger than 8

Model	Interference location ($x/B, y/B$)	U_r
SQ	(-1.5, 0.0)	11.6, 12.4
	(-2.0, 0.0)	12.4
	(1.5, 1.5)	11.6, 12.4
	(2.0, 2.0)	10.8, 11.6, 12.4
TA	(-1.5, 0.0)	10.8, 11.6, 12.4
	(1.5, 1.5)	12.4

Fundamental modal information of the three principal models is listed in Table 1. The fundamental frequencies in along-wind (longitudinal) and across-wind (lateral) directions are tuned to 6.5 Hz based on free vibration tests. The damping ratios are kept under or equal to 1% in both directions for three models and the generalized masses are about 0.11 kg. The corresponding mass-damping parameter is determined by

$$\delta = \frac{M \xi}{\rho B^2 H} \quad (1)$$

where ρ is the air density. M is the generalized mass. ξ is the damping ratio. For the rigid base-pivoted aeroelastic model in this study, the mass-damping parameters for three models are in the range of 0.23 to 0.33, which is slightly lower than the range of typical full scale high-rise buildings (0.4 – 0.6) and can be converted to Scruton numbers of 0.7 to 1.0 based on the linear mode shape assumption of its rigid elastic feature. Generally speaking, in this range of lower Scruton numbers, the across-wind

response of an isolated square prism model will increase significantly when the reduced velocity rises to values larger than 9 or 10. Furthermore, from Table 1, the parameters in these three models are intentionally made the same or similar in order to reduce the possible differences in reducing wind forces or dynamic response not by the shape changes. In real situations, the tapered building may be stiffer than the square buildings. The displacement signals of both directions are recorded by two laser sensors at the sampling rate of 550 Hz. The sampling length is 16,384 for one sample record and the ensemble size is 10 in order to obtain a statistical result.

The interfering building model is made of acrylic and has the identical size as the square prism model; unlike the principal building models, however, this interfering model is made rigid and un-flexible providing only the disturbed flow coming from upstream or downstream. The interference locations of interest are focused on those considered significant in the surrounding area (Fig. 4). Both the principal and interfering models are orientated with one face normal to the wind when both tests are carried out. Five location series including the upwind series, the oblique-upwind series, the side series, the oblique-downwind series and the downwind series are selected for observing different interference mechanisms.

RESULTS AND DISCUSSIONS

For convenient illustration hereafter, the RMS response, the standard deviation value of displacement, at rooftop is normalized to the averaged model width (0.07 m) for each sample record. The ensemble averaged RMS responses are then calculated. Among all the measurements, the averaged variation coefficients of ensemble averaged RMS responses are lower than 10% for along-wind and across-wind directions, which are both considered quite stable for the measurement accuracy. The reduced velocity is calculated as

$$U_r = \frac{\bar{U}_H}{f_0 B} \quad (2)$$

where \bar{U}_H is the mean wind velocity at the model height. In this study, 20 locations for interfering model and 11 reduced velocities ($U_r = 2.5, 3.9, 5.2, 6.8, 7.6, 8.4, 9.2, 10.0, 10.8, 11.6, \text{ and } 12.4$) together provide a total of 220 cases for the interfered response characteristics for each principal building. Among these cases, some at higher reduced velocities may be indicated to contain distorted signals in few records. In such conditions, these distorted records are neglected and the rest of records are used for further analysis. The reason of such distorted signals can be explained by Fig. 5. (Lo et al. 2016). In those failed cases, the signal was distorted simply because the laser sensor misses the target of the gimbal. For instance in Fig. 5, when the across-wind response is severe, the laser may not be able to detect the along-wind response and then resulted in distorted signals. However in this study, if the number of the distorted records is larger than 8, meaning that only two or less are left for the calculation of the ensemble averages, then such case is directly neglected. Table 2 lists the neglected cases. It is important to notice that even though these cases are neglected for comparison, their tendencies are consistent with those well-performed ones.

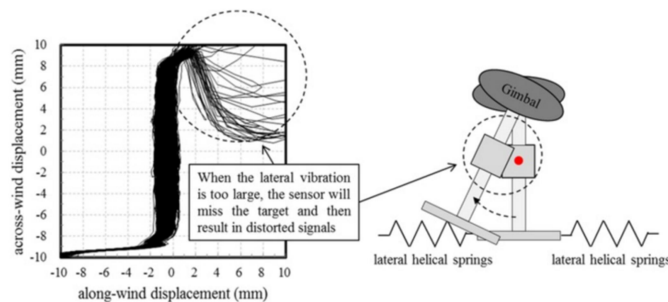


Fig. 5 Illustration of distorted signal due to laser missing

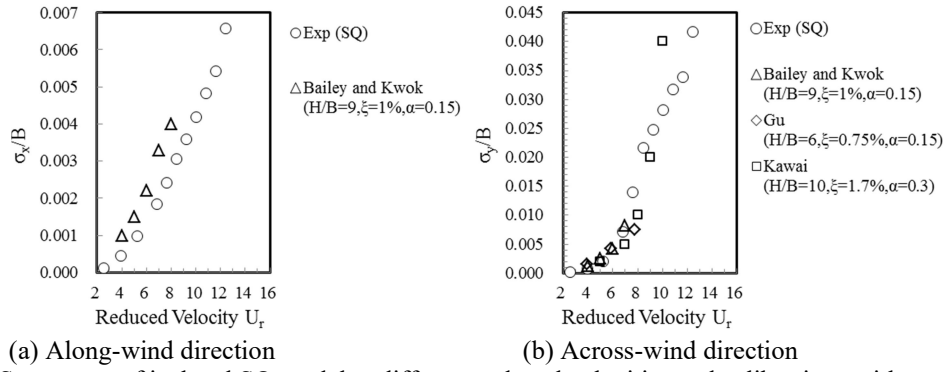


Fig. 6 RMS response of isolated SQ model at different reduced velocities and calibrations with previous works

Isolated Model

The case of the isolated square prism model (SQ hereafter) is used to demonstrate the general vibration behavior at different reduced velocities without interference effects. SQ is also for the calibrations with those square prism models in previous works to show the measurement quality of the experiments. The across-wind (lateral) RMS response at the rooftop of the isolated model exhibits the commonly known vortex-induced vibration phenomena due to its small mass-damping parameter in Fig. 6 (Bailey and Kwok, 1985; Kawai, 1992; Gu, 2005). The vibration is increased severely by increasing reduced velocity and the tendency is consistent with previous works. On the other hand, the along-wind (longitudinal) RMS response is relatively small and can be predicted to be proportional to the square of reduced velocities. Experimental results in both directions do not exactly fit to those in previous works owing to the slight differences in approaching wind and fundamental modal information.

Fig. 7 shows the responses of three isolated models under different reduced velocities. It is clearly indicated that the treatments of aerodynamic modifications perform well to reduce the dynamic responses in both directions. For the tapered model (TA hereafter), the shrinkage of cross section from the bottom to the top has successfully lowered the along-wind responses at every reduced velocity as well as the across-wind responses at higher reduced velocities. The modification provided by the TA model is considered a single modification in this study. With the addition of the helical twisting feature in the third model (the helical tapered model, TH hereafter), the across-wind responses was largely lowered to almost the same order of the along-wind ones. A constant across-wind response value is observed around the reduced velocity of 12. This modification provided by the TH model is considered to be a multiple modification. Both modification features by the TA and the TH models have proven capable of efficient wind force reduction (Kim et al., 2015).

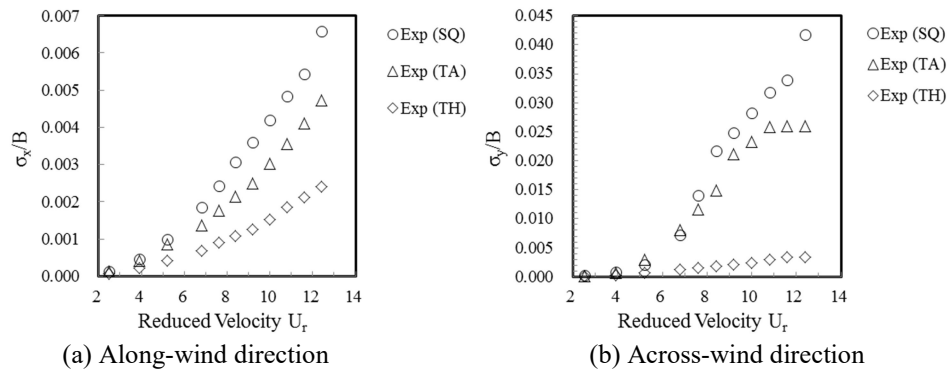


Fig. 7 RMS response of three isolated models at different reduced velocities

Upwind Series

The along-wind and across-wind responses of those interfered cases at upwind locations are shown in Fig. 8. The existence of the interfering model results in larger fluctuating responses in the along-wind direction when the relative distance is larger than $2B$ for three models. The treatment of aerodynamic modification by the TA model seems no obvious benefit as long as there is an interfering model in the upstream. The treatment by the TH model generally reduce one thirds of response when there is an interfering model in the upstream and about half of response when it is isolated. On the other hand, two opposite effects are indicated in the across-wind responses. For the SQ and TA cases, the interfering model in the upstream efficiently lowers the responses of the principal models. The closer the distance between the principal model and the interfering model, the more the response is being reduced. However, the upstream interfering model in the TH cases slightly amplifies the response of the principal model. The amplification level increases in proportional to the distance between the principal model and the interfering model. The existence of the interfering model seems to disturb the function of the twisting feature and slightly enlarges the responses in the across-wind direction.

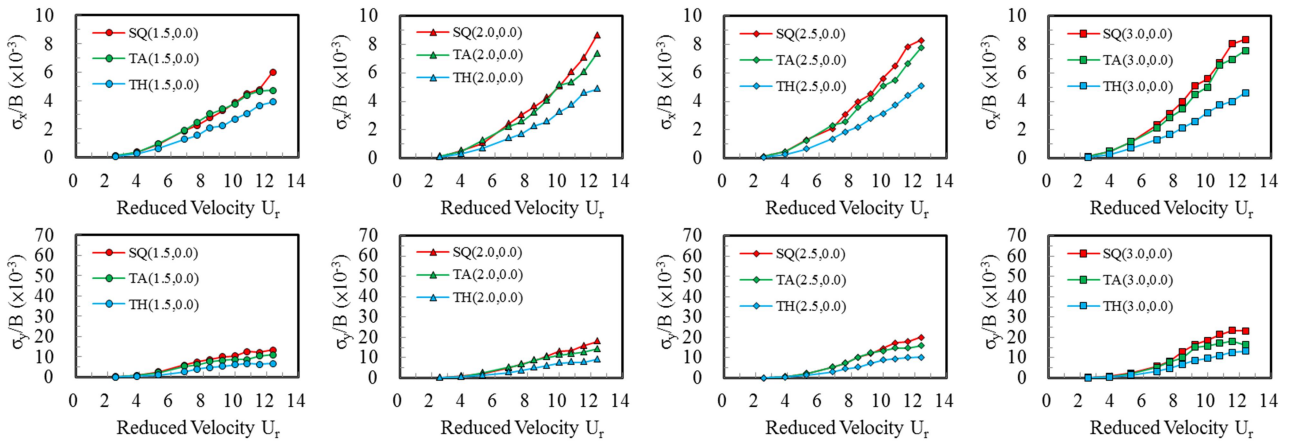


Fig. 8 Along-wind and across-wind responses for upwind location series

Oblique-upwind Series

For those cases with the interfering model at oblique-upwind locations shown in Fig. 9, the along-wind figures have similar tendencies as those at upwind locations; however, the reduction in response by the TA and TH models is more obvious than Fig. 8, especially when the relative distance is larger than $2.5B$. The across-wind figures exhibit quite interesting consequences. For the SQ and TA cases, the relative distance significantly affects the response with respect to reduced velocities. When the SQ and the TA models are isolated, the treatment of aerodynamic modification is clearly indicated when the reduced velocity is larger than 8. However, when the interfering model is located at $(1.5, 1.5)$, the treatment provided by the TA amplifies the across-wind response slightly when the reduced velocity is larger than 8. When the interfering model moves to $(2.0, 2.0)$, there is no reduction in the across-wind response by the TA model. As the relative distance increases, i.e. the interfering model moves to $(2.5, 2.5)$ and $(3.0, 3.0)$, the benefit from the treatment of the TA model shows again as the isolated cases. Comparing to the SQ and TA models, the TH model shows a generally good performance in response reduction. The across-wind response shown in the TH cases are almost in the same order of the along-wind response. Moreover, the relative distance between the principal model and the interfering model does not have an apparent effect as those in the SQ and TA cases. A sensitive relative distance between $(1.5, 1.5)$ to $(2.0, 2.0)$ may be recognized for significant interference effect. Within this range, the treatment by the TA model cannot reduce the across-wind response; instead, the response may be amplified. To eliminate such significant interference effect coming from the oblique-upwind locations, the helical twisting feature can be a good suggestion. However, in the real world, the twisting feature could also result in unfavourable construction cost.

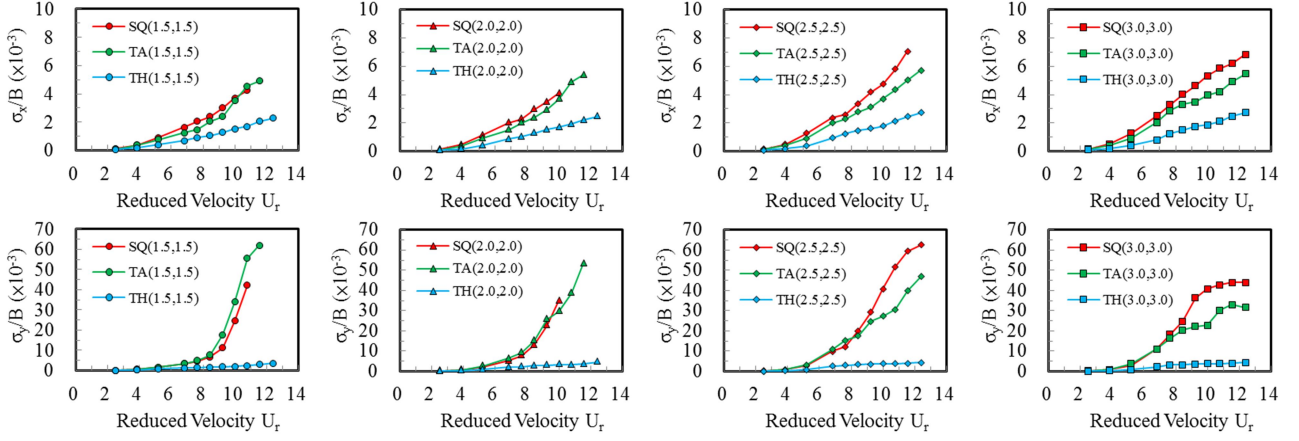


Fig. 9 Along-wind and across-wind responses for oblique-upwind location series

Side Series

For those cases at side locations shown in Fig. 10, the two treatments of aerodynamic modifications have apparent effect on along-wind responses. However, the interference effect is seldom indicated. On the other hand, not only the aerodynamic modifications but also the existence of the interfering model significantly lowers the across-wind response. It is worth noticing that the interference effect makes quite different patterns for upwind series, oblique-upwind series, and side series in the across-wind responses. The combination with the aerodynamic modification certainly changes how the interference mechanisms work.

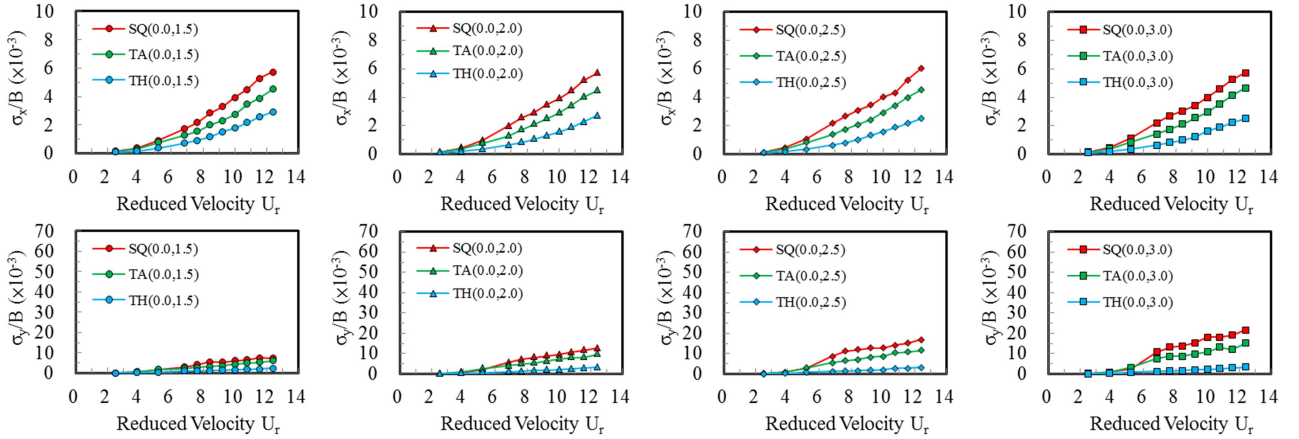


Fig. 10 Along-wind and across-wind responses for side location series

Oblique-downwind Series

The tendencies of the oblique-downwind series in Fig. 11 are very similar to those of the side series. Interestingly, the SQ case at (-1.5, 1.5) has a slightly larger along-wind response when the reduced velocity is near 5.2 – 6.8. This interference location has been introduced to exhibit an elliptic resonant-like vibration motion (Bailey and Kwok, 1985; Lo et al., 2016). The along-wind and across-wind responses have a high correlation to the rhythmic narrowing space caused by the principal model. However, this phenomenon is soon eliminated by either increasing the reduced velocity or adding the treatment by the TA model.

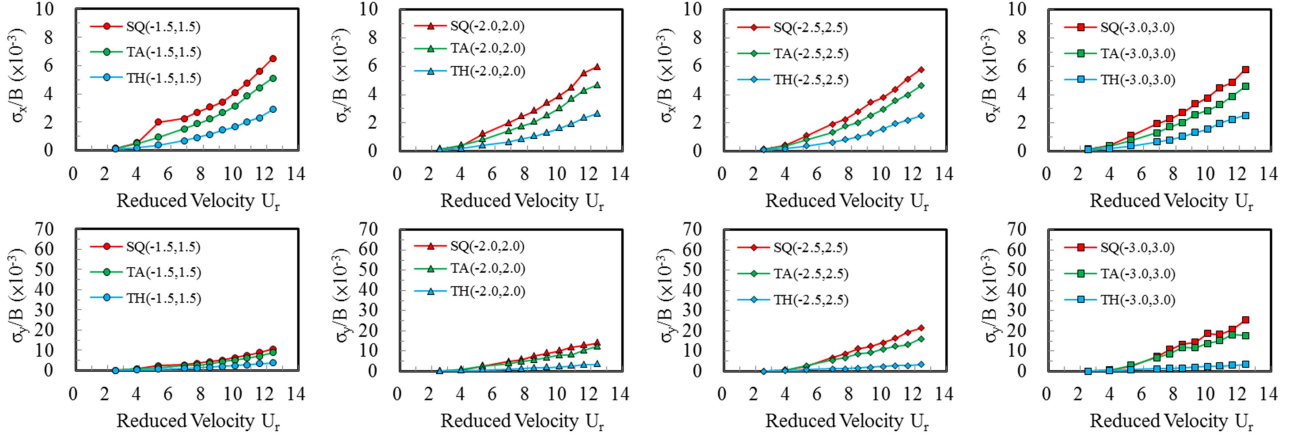


Fig. 11 Along-wind and across-wind responses for oblique-downwind location series

Downwind Series

For the downwind series, the across-wind response is affected significantly by the downstream interfering model when the reduced velocity is at higher reduced velocities. The SQ case at $(-1.5, 0.0)$ has a severe vibration when the reduced velocity is larger than 10.8; the same case at $(-2.0, 0.0)$ is similar when the reduced velocity is larger than 11.6. With the treatment by the TA model, the across-wind response at $(-2.0, 0.0)$ at every observed reduced velocity is lowered down. However, the across-wind response at $(-1.5, 0.0)$ was failed to record when the reduced velocity is larger than 10.0. For the TH cases, the across-wind responses have been amplified by the interference effect; however, unlike the cases in upwind locations, the increasing relative distance results in decreasing amplification in across-wind response. When the location is at $(-3.0, 0.0)$, no interference effect is observed coming from the downstream model.

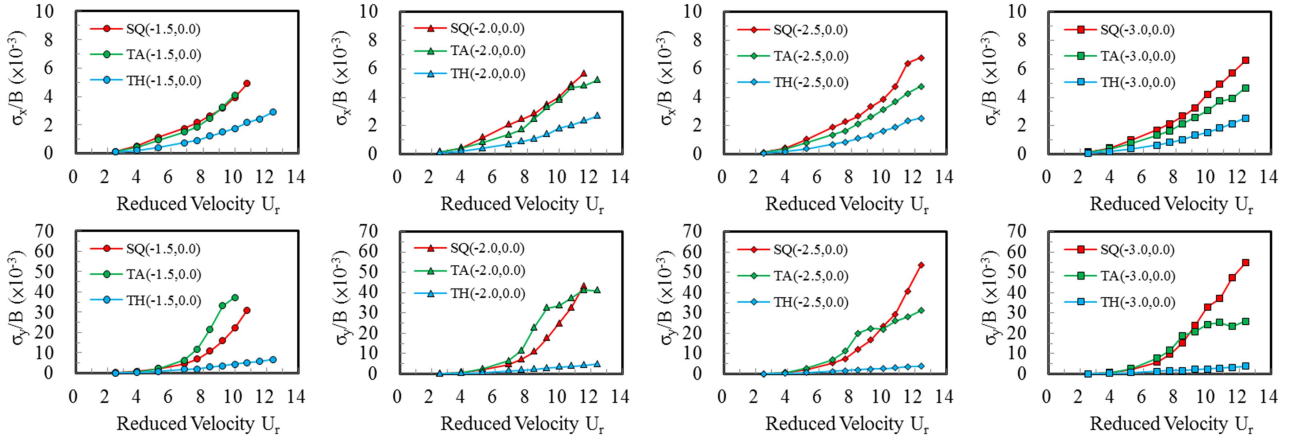


Fig. 12 Along-wind and across-wind responses for downwind location series

General Comparisons of Aerodynamic Modifications in Buffeting Factor (BF)

The efficiencies of the aerodynamic modifications provided by the TA and TH models are examined by a proposed factor with little modifications. The buffeting factor (Saunders and Melbourne, 1979) is used to evaluate how efficient the aerodynamic modification work on reducing dynamic response and is also modified as Eq. (3).

$$\Delta BF_x = \left(\frac{\sigma_x \text{ in TA or TH}}{\sigma_x \text{ in SQ}} - 1 \right) \times 100\% \quad \Delta BF_y = \left(\frac{\sigma_y \text{ in TA or TH}}{\sigma_y \text{ in SQ}} - 1 \right) \times 100\% \quad (3)$$

where σ_x and σ_y are RMS responses in the along-wind and across-wind directions respectively. Here again the numerator and the denominator are in the same interfering condition including the isolated cases. Fig. 13 shows the calculated results of Eq. (3) for all cases.

ΔBF_x in the Along-wind Response

In general, the along-wind response has been reduced by the single and the multiple treatments of aerodynamic modifications. The combination of the helical twisting provides a much better efficiency. The treatment by the TA model has different effect with respect to the interference location series. When the interfering model is located at upwind locations, the treatment does not always work well; moreover, the existence of the interfering model may reduce the reduction level by the treatment at certain reduced velocities. There is no obvious benefit indicated at upwind location series. However, for the other location series, the treatment by the TA model generally performs well except for few cases, such as (1.5, 1.5) and (-1.5, 0.0) at high reduced velocity or (-2.0, 2.0) at reduced velocity around 4. As mentioned in previous sections, these cases are referred to critical interference locations in many publications. On the other hand, the treatment by the TH model exhibits fairly good efficiency in along-wind response with the existence of the interfering model.

ΔBF_y in the Across-wind Response

The treatment by the TA model has rather complicated consequences with the consideration of different interference location series. Generally speaking, the treatment by the TA model at upwind, side, and oblique-downwind locations amplifies the across-wind response at lower reduced velocity range, say 4 to 6 from figures and reduced the across-wind response at higher reduced velocity range. When the interfering model is at oblique-upwind locations, quite complicated tendencies are produced by the treatment by the TA model and the relative distance to the interfering model. When the relative distance to the interfering model is decreasing, the case which produces the largest amplification in across-wind response moves to higher reduced velocity. For instance, when the interfering model is located at (3.0, 3.0), the largest amplification occurs at reduced velocity of 5.2; when the interfering model moves to (1.5, 1.5), the largest amplification is indicated at reduced velocity of 10. Such tendency is also found in the downwind location series with a clearer variation of the largest amplification case.

On the other hand, the performance of the treatment by the TH model is again, fairly good to reduce the across-wind response. It is worth pointing out that, the treatment by the TH model reduces the reduction level in both along-wind and across-wind responses when the interfering model is at upwind location series. It is clearly concluded from Fig. 20 that the benefit from the aero-elastic test could provide abundant information on how much the reduction level in response the treatments of aerodynamic modification produce and how the interfering model affect the results at various reduced velocities.

CONCLUSIONS

Several findings have been concluded as follows: (1) Aerodynamic modifications by changing the appearance of the building shape were confirmed through the comparisons in wind forces and responses without interference effects. However, it was found that at lower reduced velocities near 5.2 – 6.8, the aerodynamic modification provided by the tapered model may slightly amplify the across-wind response, which was unable to be discovered by the high-frequency force balance test in previous works. (2) The aerodynamic modification by the TA model was proven to be sensitive to the reduced velocity and the interference location. With the existence of a neighbouring building, such modification cannot guarantee the reduction efficiency but may sometimes amplify the across-wind vibration severely, especially at locations which are considered having critical interference effects. (3)

The modification provided by the TH model was proven to efficiently reduce both the wind force and the responses in general. The interference effect generated by the interfering model could amplify the response at certain location series. However, if compared to the isolated SQ model, the amplified response is still much smaller than no modification at all.

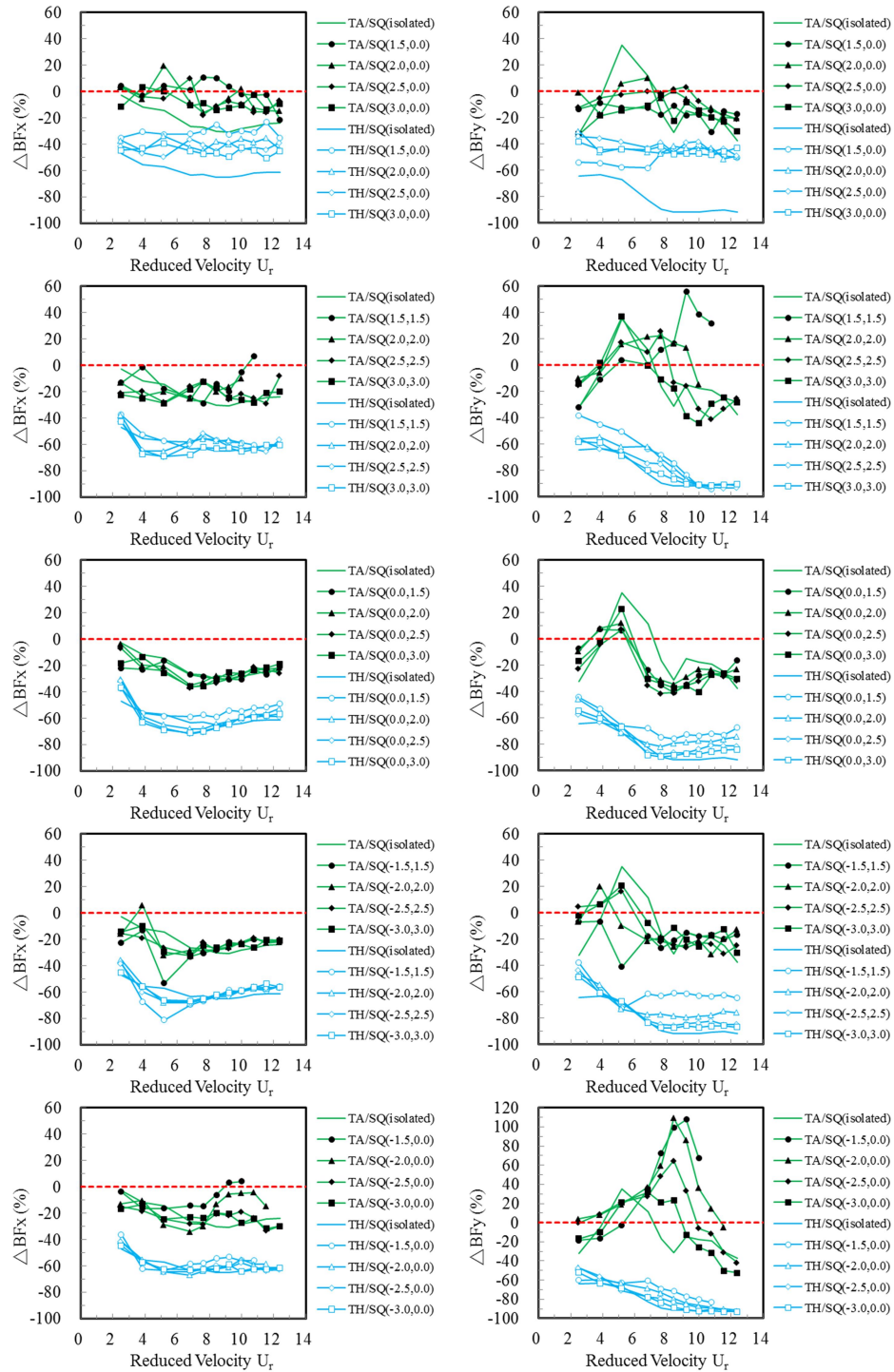


Fig. 20 Percentage distribution for response reduction efficiency against reduced velocity by aerodynamic modification

ACKNOWLEDGEMENT

Support was provided by Year 2016 Joint Usage/Research Program through Wind Engineering Research Centre in Tokyo Polytechnic University.

REFERENCES

- [1] Bailey, P.A., Kwok, K.C.S., 1985. Interference excitation of twin tall buildings. *J. Wind Eng. Ind. Aerodyn.* 21, 323-338.
- [2] Huang, P., Gu, M., 2005. Experimental study on wind-induced dynamic interference effects between two tall buildings. *Wind & Struct.* 8(3), 147-161.
- [3] Kawai, H., 1992. Vortex induced vibration of tall buildings. *J. Wind Eng. Ind. Aerodyn.* 41-44, 117-128.
- [4] Kim, Y.C., Tamura, Y., Tanaka, H., Ohtake, K., Bandi, E.K., Yoshida, A., 2014. Wind-induced responses of super-tall buildings with various atypical building shapes. *J. Wind Eng. Ind. Aerodyn.* 133, 191-199.
- [5] Kim, Y.C., Bandi, E.K., Yoshida, A., Tamura, Y., 2015. Response characteristics of super-tall Buildings – effect of number of sides and helical angle. *J. Wind Eng. Ind. Aerodyn.* 145, 252-262.
- [6] Kim, Y. C., Tamura, Y., Kim, S., 2016. Wind load combinations of atypical supertall buildings. *J. Struct. Eng.* 142(1), 04015103-1 - 04015103-8.
- [7] Lo, Y.L., Kim, Y.C., Li, Y.C., 2016. Downstream interference effect of high-rise buildings under turbulent boundary layer flow. *J. Wind Eng. Ind. Aerodyn.* 159, 19-35.
- [8] Yahyai, M., Kumar, K., Krisha, P., Pande, P. K., 1992. Aerodynamic interference in tall rectangular buildings. *J. Wind Eng. Ind. Aerodyn.* 41-44, 859-866.